IET Image Processing

Research Article

IET Journals
The Institution of Engineering and Technology

Backlit images enhancement using global tone mappings and image fusion

ISSN 1751-9659
Received on 28th June 2019
Revised 13th September 2019
Accepted on 14th October 2019
E-First on 28th November 2019
doi: 10.1049/iet-ipr.2019.0814
www.ietdl.org

Antoni Buades[1], Jose-Luis Lisani[1] ✉, Ana Belen Petro[1], Catalina Sbert[1]

[1]Departament de Matemàtiques i Informàtica – IAC 3, Universitat de les Illes Balears, Palma, Illes Balears, Spain

✉ *E-mail: joseluis.lisani@uib.es*

Abstract: The authors present a method for the enhancement of backlit images, i.e. images in which the main source of light is behind the photography subject. These images contain, simultaneously, very dark and very bright regions. In this situation, a single tone mapping function is unable to enhance the whole image. They propose the use of several such tone mappings, some of them enhancing the dark regions while others enhancing the bright regions, and then the combination of all these results using an image fusion algorithm. Qualitative and quantitative results confirm the validity of the proposed method.

1 Introduction

Backlit images, such as the one displayed in Fig. 1-left, contain, simultaneously, very dark and very bright regions. Global enhancement techniques are unable to enhance the whole image since an improvement of the dark regions leads to over-saturation of the bright zones, while the improvement of the bright regions reduces the visibility in the dark zones. Local techniques adapt the enhancement in the spatial neighbourhood of each pixel and obtain better results. However, they tend to produce halos or excessively enhance noise and image artefacts and, in general, they are unable to increase, simultaneously, the visibility in both dark and bright image regions.

Recent works [1–3], addressing specifically the problem of backlit images enhancement, propose to combine different enhanced versions of the image by using a fusion technique. This approach permits to obtain much better results than the ones obtained with global or local methods. In this paper, we follow a similar strategy but we introduce a series of improvements that permit to obtain brighter images and better contrasted results. The main contributions of the presented method with respect to previous techniques are: use of a wider set of partially enhanced images, avoiding the need of fixed or learned thresholds to discern between dark and bright image regions; a modified fusion method where the contrast of the images is assessed using a local variance measure; the use of a sharpening step *after* the fusion process, instead of including the sharpened image in the fusion process; a new method for processing colour information, which improves the contrast of the final result. Qualitative and quantitative results confirm the superior performance of the proposed method with respect to previous fusion-based techniques.

The paper is organised as follows. In Section 2, we review the literature on image enhancement techniques; Section 3 describes the proposed method; in Section 4 several experiments are displayed, alternative implementations of the proposed method are discussed and qualitative and quantitative comparisons with the existing literature are presented. The conclusions of our study are presented in Section 5.

2 Related work

The problem of image colour enhancement has been extensively treated in the literature over the years. The most popular techniques can be classified into Retinex-inspired methods and tone-mapping methods.

Retinex-inspired methods have their origin in the Retinex theory of Land [4, 5], which tried to explain the adaptability of the human visual perception to local illumination conditions. Several different, and sometimes opposing, implementations of Retinex exist. In all the cases, the goal is to recover the reflectance of the scenes, discounting the effect of the illumination. The so-called centre/surround approaches, which include the popular Multiscale Retinex (MSR) algorithm [6, 7], compute the reflectance by subtracting to the input image a blurred version of itself. Although not usually classified as a Retinex method, automatic colour enhancement (ACE) [8, 9] may be also considered as a centre/surround technique. Results obtained by such centre/surround methods are often over-enhanced and with muted colours.

Typically, the term ‘tone-mapping’ is used in the literature to refer to those techniques that map the colours of high dynamic range (HDR) images to a more limited dynamic range, obtaining the so-called low dynamic range (LDR) images. However, many of the techniques developed for HDR images can be applied to map LDR images to new LDR images with improved brightness and contrast, For this reason, in this paper we give a more general meaning to the term ‘tone-mapping’ and we use it to include also the methods that imply just a redistribution of the pixel values over the original input range. In this sense, classical histogram equalisation and its variants [10] and other basic processing methods (gamma correction, simplest colour balance [11] etc.) shall be considered as tone-mapping techniques in our paper.

These techniques can be global, when the same tone mapping function is applied to the whole image, or local, where the mapping depends on the local neighbourhood of each pixel. Some popular global techniques are: Drago *et al.* method [12], which uses a logarithmic tone mapping adapted to the luminance characteristics of the scene; Reinhard and Devlin [13], which uses a variant of the Naka-Rushton equation that models photoreceptor responses to stimuli; in [14] Mai *et al.* use a tone curve that minimises the distortions produced by the combined processes of tone-mapping and compression. Examples of local techniques are CLAHE (contrast limited adaptive histogram equalisation [15]), MLHE (morpho-local histogram equalisation [16, 17]), LCC (local colour correction [18, 19]) and the recently introduced LogLocal method [20]. CLAHE and MLHE adapt the histogram equalisation method to image sub-windows or connected regions of pixels, respectively; LCC and LogLocal use, respectively, gamma corrections and logarithmic mappings adapted to local neighbourhoods of each pixel.

Some tone mapping methods are specially focused on recovering the image details. This is achieved by decomposing the image at different resolution scales, the coarser ones keeping the global illumination information and the finer ones the details. The former are attenuated and the later amplified. Examples of these

Fig. 1 *Left: example of backlit image. Remark that very dark and very bright regions are simultaneously present in the image. Right: result obtained with the proposed enhancement method*

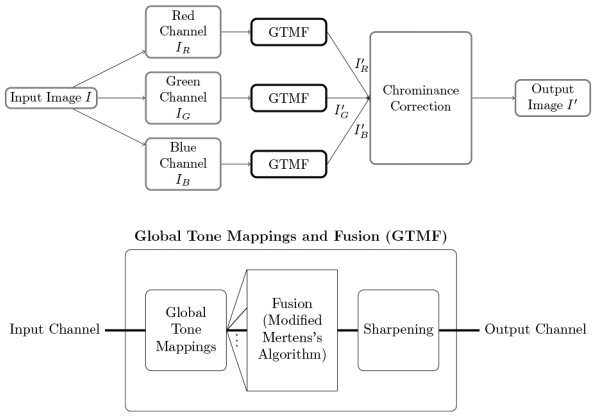

Fig. 2 *Top: block diagram of the proposed algorithm. Bottom: detail of the global tone mappings and fusion block*

techniques are Durand and Dorsey [21] and Fattal *et al.* [22] methods.

Recently, several works have focused specifically on the problem of backlit images enhancement [1–3]. All of them follow a similar approach: different enhanced versions of the original image are combined using a fusion technique. In [1], the method is applied on the V component of the HSV colour representation of the image. Three versions of the component are generated (a brighter version, a darker version and a sharpened version) and fused using Mertens's algorithm [23]. The parameters of the tone mapping functions used to obtain the darker and brighter versions of the image are tuned empirically. In [2], the original image is decomposed into illumination and reflectance. The illumination component is then processed similarly as in [1] but using a variant of Mertens's algorithm for fusion that includes a chromatic contrast term. The final result is obtained after attaching the original reflectance to the processed illumination component. Li and Wu [3] use a learning technique to segment the backlit image into frontlit (bright) and backlit (dark) regions. A different tone mapping function is applied to each region, adapted to its characteristics, and the union of the results produces the final output (a linear interpolation function is used on pixels near the borders of both regions to prevent artefacts). As the authors themselves admit, the quality of the final result heavily relies on the accuracy of the segmentation, which in turn depends on the image content.

3 Description of the method

In a nutshell, the proposed method processes independently each channel of the input image as follows: first, several tone mapping functions are applied; next, the results are combined using an image fusion technique; then, a sharpening algorithm is used to improve the contrast of the fusion result. Finally, since the independent processing of the colour channels leads to changes in chrominance with respect to the original image, a chrominance correction step is applied to recover the original colours. Fig. 2 displays a block diagram summarising the method. Fig. 1-right shows one example of application.

Our approach has similarities with [1, 2], but we propose important novelties that overcome some of the limitations of these methods, namely:

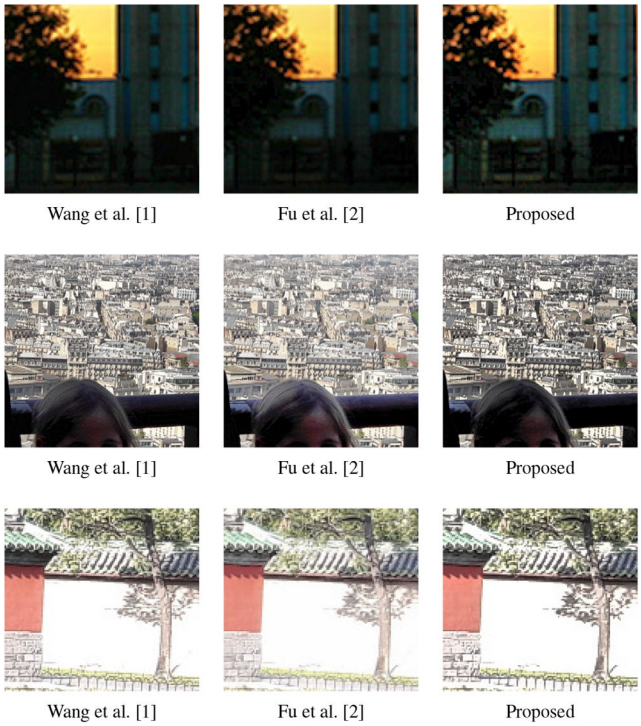

Fig. 3 *Detail of Airport, City and Paris images, where the proposed method is compared to other fusion methods in the literature*

- In [1], a gamma correction mapping is used to increase the visibility in the bright regions while a logarithmic mapping is used to improve the dark regions. In [2], an arc tangent function is applied on the original image to globally increase or decrease its luminance. In all these cases, the parameters of these functions are fixed heuristically, without a discussion on the effect of the variation of their values in the final result. We prefer the use of a set of global tone mappings (see Section 3.1) which are applied on each colour component. Some of these functions are focused on improving (i.e. brightening) the dark regions of the image while others intend to improve (i.e. darkening) the bright ones. Our approach permits greater flexibility, relying on a fusion algorithm to combine the best results of each tone mapping.
- As a way to improve the contrast of the final result, the authors of [1, 2] propose to include in the fusion process a sharpened version of the original image, computed with the GUM algorithm [24] in [1] and with CLAHE [15] in [2]. However, the fusion dilutes the sharpening effect. A better strategy, applied in the current work, is to sharpen the output of the fusion algorithm (Section 3.3). We shall see in the experimental section (Fig. 3) that our results are sharper than those of [1, 2].
- The combination of the multiple versions of the original image is performed in [1, 2] using a variation of Mertens *et al.* algorithm [23] for exposure fusion (see Section 3.2). In [1], the contribution of each image in the fused result is weighted by a factor that depends, for each pixel, on the proximity of its intensity value to the centre of the dynamic range. Values closer to the limits of this range (and presumably belonging to excessively dark or bright regions of the image) are penalised. Fu *et al.* [2] add a second weight factor that, according to the authors, measures the contrast at each pixel. The goal is to give a higher weight to more contrasted pixels, improving the contrast of the fusion result. However, they use for such measurement the chromatic filtering formula introduced in [25], which indeed measures the colour saliency of each pixel, but not its contrast. In fact, our experiments show that the contrast enhancement obtained by Fu *et al.* [2] is lower than the one obtained by Wang *et al.* [1] (see Table 1). The original fusion algorithm by Mertens already included a contrast term in the weighting factor, based on the Laplacian of the image intensity. We take up this idea but replacing the Laplacian filter (too local

and noise sensitive) by a contrast measure based on the local variance of the image.

- We propose a new way of dealing with colour images (Section 3.4). Typically, these images are enhanced by processing their luminance component and adding back the original chrominance. This guarantees the preservation of the original colours, which would be modified by the independent processing of each channel. However, we show in this paper that the application of a chrominance correction step after independently processing the colour channels produces better contrasted results.

3.1 Tone mappings

The first step of the proposed method consists in generating several versions of the original image, some of them exhibiting a contrast improvement in dark regions and some of them in bright regions. In principle, any of the global or local contrast enhancement techniques reported in Section 1 could have been used to generate this set of images. However, for the sake of simplicity we decided to use just two types of global tone mapping functions, namely, gamma and logarithmic functions. Each of them are widely used in the literature, both depend on a single parameter and they have some characteristics that make them suitable for our purposes.

Specifically, the following tone mapping functions are used to map the original values, for each colour channel and assumed in the range [0, 255], to new values in the same range

$$G(\gamma)(I) = 255\left(\frac{I}{255}\right)^{\gamma}, \gamma \in \{0.4, 0.6, 0.8, 1, 2, 3\}, \quad (1)$$

$$L(\alpha)(I) = \frac{255\log(\alpha I + 1)}{\log(255\alpha + 1)}, \alpha \in \{0.1, 0.2, 0.3, 0.4, 0.5\}, \quad (2)$$

where I refers, indistinctly, to any of the original R, G or B values.

Equation (1) corresponds to different gamma functions. These functions have the property of either increase the luminance of the dark regions or decrease the luminance of the bright regions, depending on the value of their parameter. When $\gamma < 1$ the function is concave, thus achieving a contrast improvement in the dark regions (at the expense of a decrease in contrast in the bright regions); when $\gamma > 1$ the function is convex, and the behaviour is the opposite (see Fig. 4). Therefore, with the variation of a single parameter we can generate the set of input images needed by our method. We have chosen a small set of values ($\gamma \in \{0.4, 0.6, 0.8, 1, 2, 3\}$) which cover the full range of needed transformations, including the identity function (corresponding to $\gamma = 1$), which means that the original input image belongs to the set of images used for merging. We do not consider values of γ smaller than 0.4 (resp. larger than 3) since they produce excessively bright (resp. dark) images (see Fig. 5).

Equation (2) corresponds to different logarithmic functions (remark that the output of the tone mapping does not depend on the base of the log function, because of the normalisation factor $\log(255\alpha + 1)$). These functions have been included because of their steep slope at low intensity values, which permits a greater increase of the luminance of the dark regions than the one provided by the gamma functions (see Figs. 4 and 5). The set of parameters of the function has been chosen to cover the range of transformations that permit to enhance the dark regions but without creating excessively bright images (for this reason values of α larger than 0.5 are not used). Moreover, values of α smaller than 0.1 are not considered because the results of the tone mapping are similar to the ones obtained with the gamma functions.

3.2 Images fusion

For each colour channel, the tone mapping results obtained by applying (1) and (2) are combined using a new image fusion algorithm based on Mertens *et al.* [23]. The algorithm in [23] was designed to merge several pictures of the same scene captured with different exposure times. Mertens's algorithm computes a series of quality metrics, *contrast, saturation* and *well-exposedness* for each input image.

Table 1 Average contrast values (computed with (9)) and NIQE values for a dataset of 50 images processed with different image enhancement methods

	Average contrast	Average NIQE
original	1.00	3.56
CLAHE [15]	7.01	3.09
MLHE [16, 17]	47.05	3.21
ACE [8]	2.76	3.23
LCC [18]	6.71	3.16
LogLocal [20]	6.41	3.08
MSR [6]	56.07	3.10
Drago *et al.* [12]	4.17	3.25
Wang *et al.* [1]	6.22	3.23
Fu *et al.* [2]	5.87	3.07
proposed	14.85	3.06

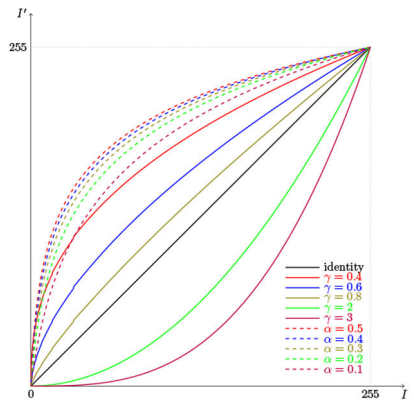

Fig. 4 *Tone mapping functions used in the proposed method. Continuous lines: gamma functions. Dotted lines: logarithmic functions*

- *Contrast C:* the absolute value of the Laplacian filter applied to the greyscale of each image.
- *Saturation S:* measures the standard deviation of the R, G and B channels.
- *Well-exposedness E:* measures the closeness to the mid intensity value using a Gaussian curve, $\exp\left(-\frac{(I/255-0.5)^2}{2\sigma_i^2}\right)$, where σ_i is a parameter that the authors fix to 0.2.

These metrics are combined into a weight map for each image

$$w_k(x) = \frac{C_k(x)^{\alpha_c} S_k(x)^{\alpha_s} E_k(x)^{\alpha_e}}{\sum_{j=1}^{N} C_j(x)^{\alpha_c} S_j(x)^{\alpha_s} E_j(x)^{\alpha_e}}, \quad k = 1, 2, \ldots, N,$$

where N is the number of images to be merged and α_c, α_s, α_e are weighting exponents.

The weight of each image at each pixel depends on its value, its colour saturation and its contrast. The goal is to prioritise values closer to the centre of the dynamic range (i.e. 127.5) which are supposed to correspond to regions neither too dark nor too bright. Moreover, more contrasted regions are preferred over uniform regions, since edges and textures are to be preserved.

The fusion result at each pixel $\boldsymbol{x}$ could be computed as a weighted average of the values of each image at $\boldsymbol{x}$

$$I'(\boldsymbol{x}) = \sum_{k=1}^{N} w_k(\boldsymbol{x}) I_k(\boldsymbol{x}), \tag{3}$$

where I_k is the kth input image and $w_k(\boldsymbol{x})$ is the weight of the kth image at $\boldsymbol{x}$.

However, the naive application of (3) leads to unsatisfactory results, due to the sharp spatial fluctuations of the weight functions, especially in the proximity of edges. Therefore, Mertens *et al.* propose a multi-resolution blending strategy based on image pyramids. They build a Laplacian pyramid for each input image and a Gaussian pyramid for each weight map, and at each level l of the pyramid the Laplacian of the fused image is computed as

$$\boldsymbol{L}^l\{I'\}(\boldsymbol{x}) = \sum_{k=1}^{N} \boldsymbol{G}^l\{w_k\}(\boldsymbol{x}) \boldsymbol{L}^l\{I_k\}(\boldsymbol{x}), \tag{4}$$

where $\boldsymbol{L}^l$ and $\boldsymbol{G}^l$ denote, respectively, the l level of the Laplacian and Gaussian pyramids.

In this paper, we propose two modifications of the fusion algorithm described above: first, and since the fusion method is applied on one channel images, the saturation term is skipped; second, the contrast measure based on the Laplacian filter is replaced by a measure based on the local variance around each pixel. This local variance is computed as the variance of the grey levels in a patch of size 7×7 centred at the pixel. The use of a neighbourhood permits to obtain a smoother contrast term than when using the Laplacian filter, and less sensitive to noise.

The proposed weight function is

$$w_k(\boldsymbol{x}) = \frac{1}{Z} \mathrm{e}^{\left(-\frac{\left(\frac{I_k}{255}-0.5\right)^2}{2\sigma_i^2}\right)} \cdot \left(\mathrm{e}^{\left(\frac{\mathrm{Var}(\boldsymbol{x})}{2\sigma_c^2}\right)} - \mathrm{e}^{\left(-\frac{\mathrm{Var}(\boldsymbol{x})}{2\sigma_c^2}\right)}\right), \tag{5}$$

where σ_i and σ_c are parameters that we fix to 0.1 and 0.2, respectively, $\mathrm{Var}(\boldsymbol{x})$ denotes the variance of the patch centred at pixel $\boldsymbol{x}$ and Z is a normalisation factor. The use of this contrast term improves the contrast of the fusion result as we shall see in Section 4.1.

3.3 Sharpening post-processing

The contrast of I' (i.e. the fusion result for a given colour channel) is globally enhanced by using a sharpening technique.

The classical unsharpening algorithm can be described by

Fig. 5 *Examples of different tone mappings applied to the image in Fig. 1-left (green component). From left to right: (2) with $\alpha = 0.5$, (1) with $\gamma = 0.4$ and $\gamma = 3$*

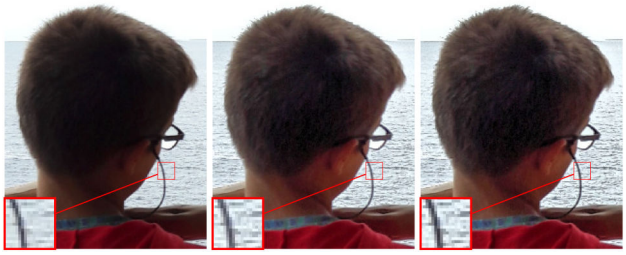

Fig. 6 *From left to right: original; result of the proposed method when no sharpening algorithm is applied after the fusion step; result when sharpening is used. The differences between the images are better appreciated in the supplementary web page*

$$I_s = L(I) + \alpha(I - L(I)),$$

where I is the input image, $L(I)$ is a low-pass version of I and α is the gain. Then, $I - L(I)$ contains the details of the image, and choosing $\alpha > 1$ the sharpness is increased.

We use the screened-Poisson equation [26, 27], to separate the details. In [26, 27], the authors propose a simple gradient domain method to eliminate the non-uniform illumination while preserving the details. The model consists on minimising the functional

$$J(u) = \int_\Omega \left|\nabla u - \nabla I\right|^2 \mathrm{d}x + \lambda \int_\Omega u^2 \mathrm{d}x, \tag{6}$$

where I is the input image and Ω the image domain. The first term of the functional J is responsible of preserving the details while the second tries to minimise the variance. Parameter λ is a constant that controls the trade-off between both terms. The function that minimises J must satisfy the Euler-Lagrange equation, known as screened Poisson equation

$$\lambda u(x) - \Delta u(x) = -\Delta I(x), \quad x \in \Omega, \tag{7}$$

with homogeneous Neumann boundary condition. In [26], the authors show that the solution of the screened Poisson equation (7) acts as a high-pass filter of I when λ increases, containing the details. The difference I - u is a low-pass version of I.

We use the screened Poisson equation (7), using I' as the input image, to obtain the details of I', which we will denote $H(I')$; the low-pass version of the image is obtained as $L(I') = I' - H(I')$. We can obtain a sharper image applying $I'_s = L(I') + \alpha H(I')$, where $\alpha > 1$ is a parameter of the method that we set to 1.25 in our implementation. Fig. 6 illustrates the different results obtained with and without the sharpening post-processing step.

3.4 Chrominance correction

As a result of the previous steps, we may get an enhanced image whose colours differs from the original, as illustrated in Fig. 7. This is due to the independent processing of each colour channel. In order to recover the original chrominance, we apply the following procedure.

We denote by $\boldsymbol{v} = (R, G, B)$ the colour vector corresponding to a pixel in the processed image, and by $\boldsymbol{v}_\mathrm{o} = (R_\mathrm{o}, G_\mathrm{o}, B_\mathrm{o})$ the colour vector of the same pixel in the original image. The corrected colour vector $\boldsymbol{v}_\mathrm{c}$ is obtained by projection of the new vector onto the direction of the original vector

$$\boldsymbol{v}_{\mathrm{c}} = (\boldsymbol{v} \cdot \boldsymbol{v}_{\mathrm{o}}) \frac{\boldsymbol{v}_{\mathrm{o}}}{\|\boldsymbol{v}_{\mathrm{o}}\|^2}$$

Remark that by using this transformation the original R/G/B ratios are kept, thus preserving in this sense the original chrominance of the input image.

Fig. 7 illustrates how the use of this technique permits to recover the original colours while keeping the enhancement in illumination.

Remark that this way of processing colour images differs from the standard procedure consisting in decoupling luminance from chrominance information (using HSV, HSI, YCbCr or other convenient colour space), then processing the luminance and finally adding back the chrominance components. In Section 4.2.2, we justify both qualitatively and quantitatively our decision.

4 Experimental results

In this section, we present several results of the application of the proposed method to backlit images. To facilitate the quantitative evaluation of the obtained results, we propose, in Section 4.1, a new measure of the local contrast improvement between original and processed images. In Section 4.2, we justify the design decisions adopted in the proposed method, comparing the results of the proposed implementation to results obtained with other possible implementations. In Section 4.3, we compare the method to other techniques in the literature.

The interested readers can test the proposed method with the online demo available at http://ipolcore.ipol.im/demo/clientApp/demo.html?id=77777000027. Moreover, the figures displayed in this section can be visualised in the following web page: http://researchtami.uib.es/backlit/supplementary/. The display format of this page permits an easy comparison between the results of the different methods.

4.1 Quantitative evaluation of the contrast enhancement

A common method to assess the contrast of an image is to compute the entropy of its histogram of intensity values. However, as we will show in this section, the entropy measure is not always able to account for actual increases in contrast. For this reason, we will propose a new measure of the variation of the local contrast obtained after applying a contrast enhancement technique to a given image. We shall use this measure to compare the performance of different processing.

Let us recall the definition of the entropy of a histogram of intensity values

$$E = -\sum_{i=0}^{L-1} p_i \log(p_i) \tag{8}$$

where p_i is the fraction of pixels having intensity i and L is the number of different intensity values ($L = 256$ for 8-bit images).

Fig. 8 illustrates the limitations of the entropy measure when assessing the difference in contrast between images. The first two images in the figure are two instances of the same original image obtained using different quantisation factors. They have a very similar contrast but their entropies are quite different (4.42 and 4.11, respectively). On the other hand, the third is obtained after applying a linear tone mapping to the second, resulting in a more contrasted image. However, both images have the same entropy 4.11.

The reason for the difference between the first and second images is that, although the images look similar, the quantisation operation modifies the distribution of intensity values, thus resulting in different p_i factors in (8) and therefore in quite different entropy values. In the case of the second and third images, the linear tone mapping (and, in general, any monotonic tone mapping) remaps the original intensity levels to new levels but preserves the ordering between them (if a pixel is brighter than another in the original image it will remain brighter also in the processed image). This implies that the p_i factors get reassigned to new intensity values, but their magnitudes remain the same. Thus, the entropy measure remains unchanged (up to numerical errors due to rounding or saturation).

Fig. 7 *Result of the chrominance correction step. From left to right: original, processing result without chrominance correction, final result of the proposed method*

Fig. 8 *Example of the limitations of the entropy measure as an indicator of the image contrast. The entropy values of the images, from left to right, are, respectively, 4.42, 4.11 and 4.11. However, the first two images are perceived as having the same contrast and the difference in contrast with the third is conspicuous. The proposed contrast measure agrees with our perception: the contrast is almost the same between the first and second images $C = 1.05$, while it is higher for the third image when compared to the second $C = 1.32$*

We propose the following measure which faithfully measures the variation in contrast produced by the processing

$$C = \frac{1}{N} \sum_{k=1}^{N} \frac{\mathrm{Var}_k^{\mathrm{processed}}}{\mathrm{Var}_k^{\mathrm{original}}} \tag{9}$$

where Var_k denotes the variance of the intensity values in a patch of size $s \times s$ (typically we use $s = 16$). This variance is computed, on both the original and processed images, over all the $s \times s$ patches contained in the images' domain. N denotes the number of patches used in each image. The proposed measure is simply the average ratio of these variances over all the patches. Values greater than one indicate a contrast improvement, while values equal or smaller than one indicate that the processed image has a similar or inferior contrast than the original.

By applying this measure to the images in Fig. 8, we obtain values of $C = 1.05$ between the first and second images (indicating a very small difference in contrast) and $C = 1.32$ between the second and third (indicating a considerable increase in contrast). These results agree with our perception.

4.2 Discussion of the proposed method

This section analyses the configuration and implementation of the method described in Section 3 and summarised in Fig. 2. We show with qualitative and quantitative results that the proposed choices outperform other possible method configurations.

We analyse different aspects of the proposed method:

- The application of the method to colour images. We compare with two different strategies: direct application of the fusion step to colour images, without decoupling the channels (Section 4.2.1); and application of the method only to the luminance channel, after applying a luminance-chrominance decorrelation transform (Section 4.2.2).
- The choice of the contrast term for the fusion method (Section 4.2.3).
- The sharpening post-processing step (Section 4.2.4).
- The parameters of the method (Section 4.2.5).
- The use of alternative fusion algorithms (Section 4.2.6).

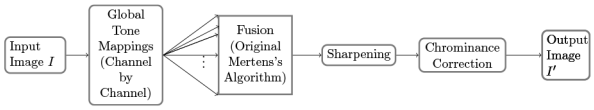

Fig. 9 *Block diagram of the alternative algorithm discussed in Section 4.2.1*

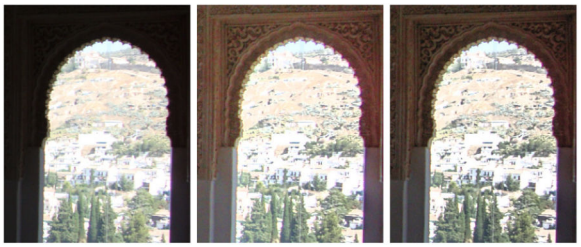

Fig. 10 *From left to right: original; result of after applying the fusion algorithm to tone-mapped colour versions of the original; result of the proposed approach. The contrast enhancement (computed with (9)) is 4.84 for the first method and 5.20 for the second*

Fig. 11 *From left to right: original, result of processing the V channel and adding back the original HS components, result of independent processing of RGB channels and chrominance correction*

4.2.1 Fusion of colour images: Fig. 9 displays a variation of the proposed method in which the different tone mappings (1) and (2) are applied to the original colour image (channel by channel) and the obtained results are then merged using Mertens's exposure fusion algorithm (as described in [23]). Remark that this is different from what we actually propose in Section 3, where the tone mappings and fusion steps are applied channel by channel, i.e. on monochrome images (see Fig. 2).

Fig. 10 shows one example of the difference between the results of both approaches. We observe in this case that the contrast is better with the proposed method, even though with the alternative approach the image is slightly brighter. The contrast enhancement with respect to the original (measured with (9)) is $C = 4.84$ for the alternative method and $C = 5.20$ for the proposed approach. We computed the average contrast enhancement over a set of 50 images and we obtained $C = 10.39$ when fusing tone-mapped colour images and $C = 14.85$ when fusing monochrome images as proposed. These results support the validity of the chosen method.

4.2.2 Processing of intensity channel: It is well known that independently processing the channels of a colour image leads to (generally undesirable) changes in its chrominance. For this reason, many contrast enhancement methods are applied just on the luminance component of the image (e.g. V when using the HSV colour space, as in [1]; or I when using HSI) and the original chrominance components are added back to the processed luminance in order to obtain the final colour image.

We will show in this section that the image contrast is further improved when the contrast enhancement is applied independently on each channel and the original chrominance is recovered afterwards.

Let us begin with a toy example (Fig. 11) where the result of processing the V component of a colour image and adding back its original H and S components (as described in the block diagram of Fig. 12) is compared to the result of independently processing each channel and then recovering the original chrominance as described in Section 3.4. We can see clearly that the image is more contrasted and the colours more vivid in the second case. The reason is that the value of V is the same in both colour bands, therefore both

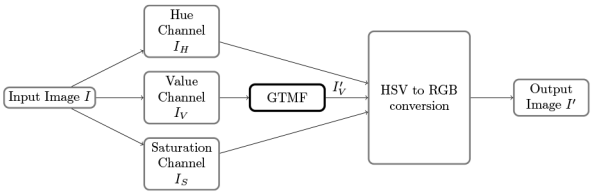

Fig. 12 *Block diagram of the alternative algorithm discussed in Section 4.2.2. The GTMF block is the same displayed in Fig. 2*

Fig. 13 *From left to right: original; result of processing V channel and adding back original HS components; result of independent processing of RGB channels and chrominance correction*

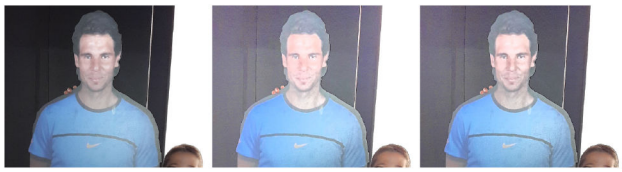

Fig. 14 *From left to right: original; result of the proposed method when using, in the fusion algorithm, the Laplacian as a measure of the image contrast; result when using the local variance. The contrast enhancement (computed with (9)) is 1.94 for the first method and 2.12 for the second*

regions are processed the same way by the first method. By independently processing each channel we obtain a better contrasted result.

The same is true for any natural image, such as the one displayed in Fig. 13. We observe again a better contrast and more vivid colours when using the proposed technique. In order to quantitatively measure the contrast improvement, we computed the average contrast enhancement C (9) over a set of 50 images and we got $C = 6.96$ when processing the V channel and $C = 14.85$ when processing each channel, which confirms the validity of the proposed procedure.

4.2.3 Contrast measurement in fusion method: Fig. 14 displays the result of our method when using, in the image fusion algorithm, the contrast measure based on the Laplacian (originally proposed by Mertens *et al.* [23]) and the one proposed in this paper, based on the local variance. We observe that the contrast is better in the second case, which is confirmed by the contrast measure C (9): $C = 1.94$ in the first case; $C = 2.12$ in the second case.

We computed the average contrast enhancement C over a set of 50 images and we got $C = 14.55$ when using the Laplacian measure and $C = 14.85$ when using the local variance.

4.2.4 Analysis of the sharpening post-processing: Fig. 6 compares the results of our method without (central image) and with (right image) the application of the sharpening step after the fusion algorithm. The image looks crisper in the latter case. The difference is better appreciated in the web page created as supplementary material for this article.

In general, the use of the sharpening step permits to obtain more contrasted results. Over a set of 50 images, the average contrast (computed with (9)) is $C = 11.34$ without sharpening and $C = 14.85$ with it.

4.2.5 Parameters of the method: The proposed method depends on several parameters that have been fixed once and for all the experiments shown in the previous sections and in Section 4.3. Here we summarise them and discuss how their variation influences the obtained results. These parameters are:

- γ and α values for the gamma and log functions described in Section 3.1. They have been chosen across the range of possible values so that not too dark or too bright images are used in the fusion process. The default sets of values are $\gamma \in \{0.4, 0.6, 0.8, 1, 2, 3\}$ and $\alpha \in \{0.1, 0.2, 0.3, 0.4, 0.5\}$. Fig. 15 compares the results of using these default values with the ones obtained with the sets $\gamma' \in \{0.2, 0.3.0.4, 0.6, 0.8, 1, 2, 3, 4, 5\}$ and $\alpha' \in \{0.05, 0.1, 0.2, 0.3, 0.4, 0.5, 0.6, 0.7\}$. These new values imply that very bright and very dark images are fused together. The difference with respect to the results obtained with the default values are especially noticeable in the dark regions of the image, where noise and small artefacts become excessively enhanced, as can be seen in the figure.
- σ_i and σ_c, used in (5) and that influence the result of the fusion method described in Section 3.2. We refer to [28] for a detailed discussion of the parameters of Mertens's fusion algorithm. This paper shows that the optimal range of values for σ_i is [0.1, 0.2], since for values outside this range the fusion result is a mere average of the input images. The parameter σ_c controls the importance of the image's contrast in the merging. If σ_c is high the weight factor is linear with the contrast, and as σ_c decreases only the highest contrasted images are used for merging. However, if the value is too low, we end up obtaining a simple average of the inputs. In our tests, values of σ_c in the range [0.1, 0.4] provided good results, and we have fixed the default value to 0.2. Fig. 16 compares the results obtained with different values of σ_c.
- α and λ, used for the sharpening post-processing described in Section 3.3. The value of λ has been fixed to 0.1, according to the recommendations of the authors of [26, 27]. For α we use the value 1.25. Excessively high values of this parameter produce halos and artefacts in the final result (see Fig. 17).

4.2.6 Alternative fusion techniques: The fusion method described in Section 3.2 has been chosen for its simplicity and because it permits to take into account the local contrast of the images into the fusion process (through (5)). In Section 4.2.3, a comparison between our results and the ones obtained using Mertens's original fusion algorithm [23] has been performed, but several other fusion techniques have been proposed in the literature in recent years. We have compared our results with those obtained by replacing the proposed fusion method by the ones proposed in [29, 30]. In general, we observe that the contrast is better enhanced by our method. Moreover, the method in [29] tends to produce halo artefacts. An example of the obtained results is shown in Fig. 18. A comprehensive comparison with other fusion techniques is out of the scope of the current paper and shall be the subject of a future research.

Fig. 15 *From left to right: original; result of the proposed method when using the default parameters; result when using a different set of γ and α values for the tone mappings. In the dark regions, noise and image artefacts get excessively enhanced*

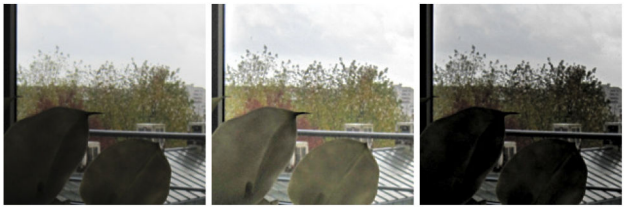

Fig. 16 *From left to right: original; result of the proposed method when using the default parameters; result when using $\sigma_c = 0.05$ in the fusion process*

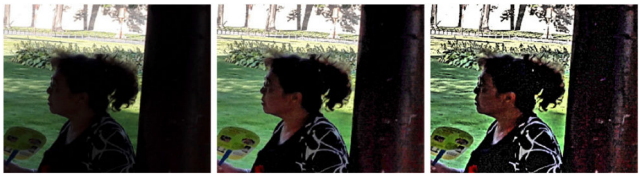

Fig. 17 *From left to right: original; result of the proposed method when using the default parameters; result when using $\alpha = 3$ in the sharpening post-processing. Halos and artefacts can be observed in the result*

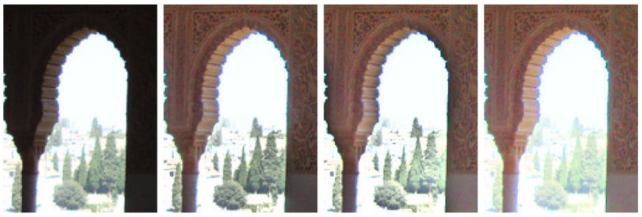

Fig. 18 *From left to right: original; result after applying the proposed fusion algorithm; result using the fusion method described in [29]; and result applying the method from [30]. The contrast enhancement (computed with (9)) of the respective results is 23.59, 15.37 and 12.25*

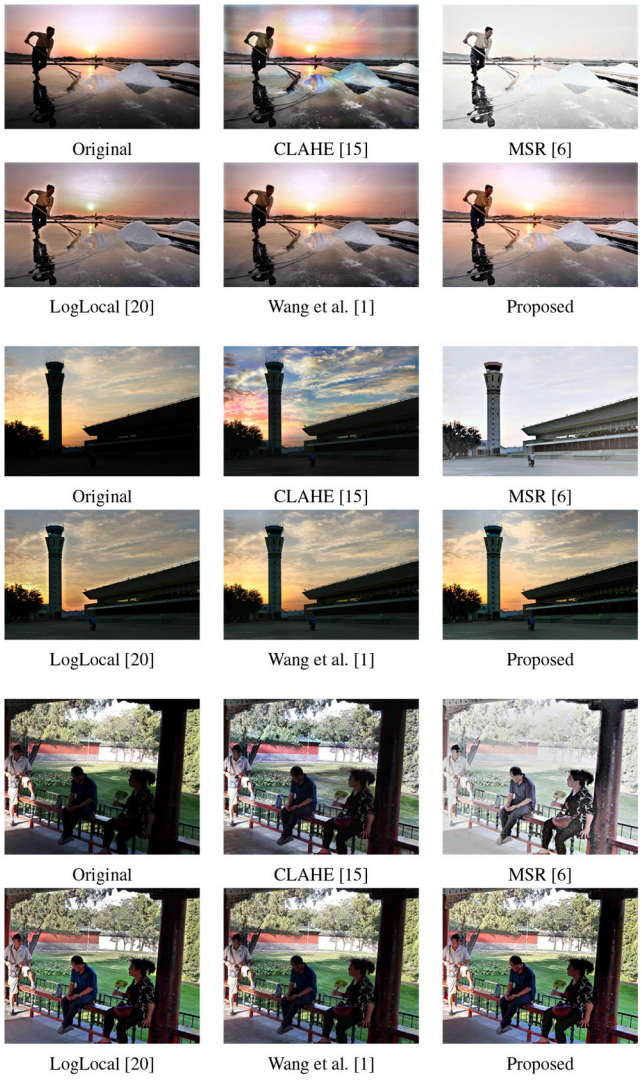

Fig. 19 *Comparison of results of different contrast enhancement methods. From top to bottom, images Salt, Airport and Garden*

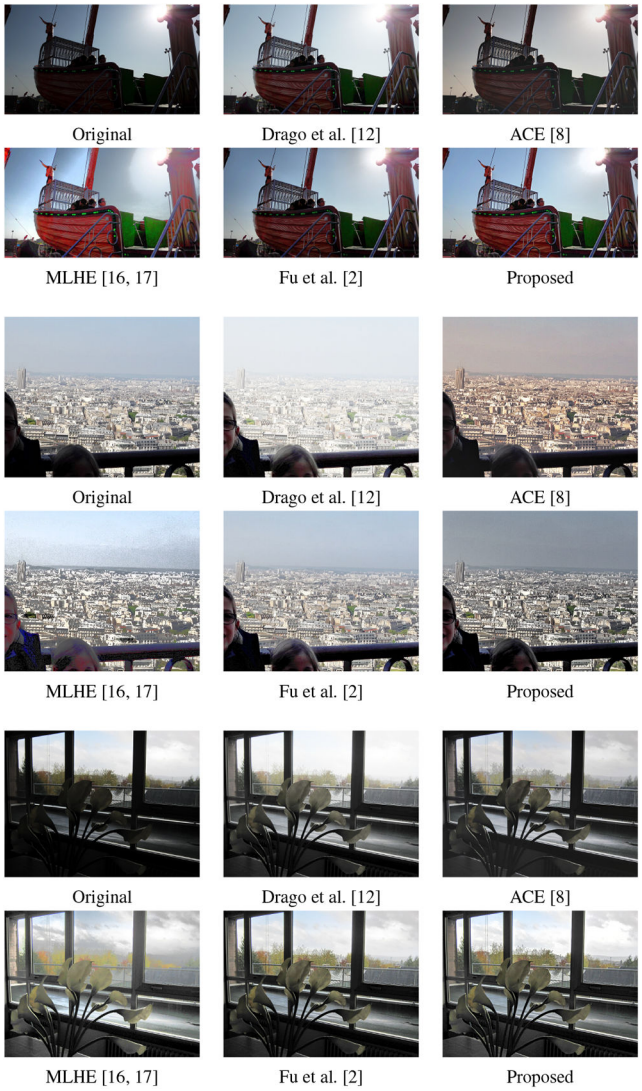

Fig. 20 *Comparison of results of different contrast enhancement methods. From top to bottom, images Viking, City and Iris*

4.3 Comparison with other methods

We have compared the results of the proposed method with the results obtained with many popular contrast enhancement techniques: CLAHE [15], MLHE [16, 17], MSR [6], ACE [8], LCC [18], LogLocal [20], Drago *et al.* [12], and two recent fusion-based techniques by Wang *et al.* [1] and Fu *et al.* [2].

Figs. 19 and 20 display some of the obtained results. In general, MSR produces excessively saturated images with muted colours, MLHE and CLAHE over-enhance the noise and compression artefacts (see Fig. 21) and Drago *et al.*'s method is unable to enhance simultaneously dark and bright regions. The results obtained with ACE, LCC and LogLocal are good in general, although ACE and LCC produce darker images than our method and LogLocal suffers from halo artefacts (see Fig. 22).

The best results are obtained with methods based on image-fusion techniques ([1, 2] and our proposal). In Fig. 3, we compare some details of the results obtained with the three methods. We observe that the highest improvement in contrast is obtained with the proposed method, although our results may be slightly oversaturated in bright image regions that contain well-contrasted objects. See for instance, the clouds in Fig. 19 (Airport image) and Fig. 20 (Iris image).

In order to quantitatively evaluate the performance of the proposed technique, we compute the contrast (measured with (9)) and the NIQE blind image quality assessment index [31] over a set of 50 images for the different enhancement methods. NIQE measures deviations from statistical regularities observed in natural images, lower values of this index indicate higher quality images. The results are displayed in Table 1.

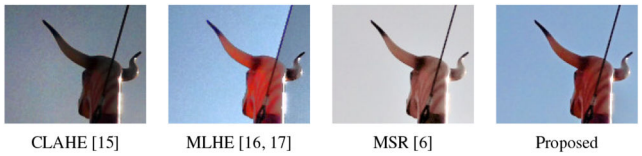

Fig. 21 *Detail of Viking image*

The contrast enhancement obtained by the proposed method is higher than the one achieved with most of the other compared techniques. Only MSR and MLHE obtain better results. However, as commented above, these methods either produce excessively saturated images (MSR) or they enhance excessively noise and image artefacts (MLHE). Our method enhances the contrast but preserves the visual quality of the results, as confirmed by the NIQE measure, for which the proposed technique obtains the best score. It must be remarked that the qualitative results shown in the previous figures do not always agree with the obtained NIQE values. For instance, CLAHE obtains the third best value of the index but, visually, the results are not always good (as shown in Fig. 21). A similar comment applies to MSR. On the other hand, LogLocal produces good quality results but the contrast is lower than with the proposed method. A similar remark applies to Fu *et al.* method.

We conclude this section with an example of the adaptation of the proposed method to multi-exposure images. Indeed, although our method has been designed to work with simulated multi-exposure images, obtained from the original input through several

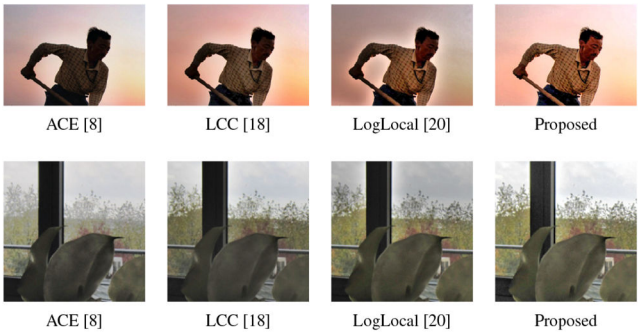

Fig. 22 *Detail of Salt and Iris images*

Fig. 23 *Top: three of the multi-exposure input images used in the experiment. Bottom, from left to right: result of the fusion and sharpening techniques proposed in this paper; result from [29]; result from [32]*

tone mappings, it is possible to apply the fusion and sharpening steps on real multi-exposure images. However, it must be remarked that the parameters of these steps have not been optimised for this kind of input. Moreover, since there is not a single input image, it is not clear which one of the inputs shall be used as reference for the chrominance correction step. In Fig. 23, we compare our result with the ones obtained with two state-of-the-art methods, designed specifically for this kind of problem [29, 32]. For this example we applied, on a channel by channel basis, the fusion and sharpening techniques described in Sections 3.2 and 3.3, but the chrominance correction step was skipped. We observe that the contrast of the obtained image is good but the colours are less saturated than in the other results.

5 Conclusions

We have proposed a new image enhancement technique that is able to cope, simultaneously, with dark and bright regions of the image. The technique is based on fusing the results of several tone mappings applied on the original colour channels. Contrarily to other enhancement methods that use image fusion techniques, we do not fuse just two versions of the original image, one improving the dark regions and the other the bright regions. Instead, we use a whole family of tone mappings and we adjust the parameters of the fusion method so that the local brightness variance in the final result is increased, which guarantees an improvement in contrast. Moreover, we propose a new way of processing colour information which further improves the contrast of the final result. The experimental results show that, in general, the images obtained with the proposed method are brighter and more contrasted than those obtained with other techniques.

6 Acknowledgments

The authors were supported by grants TIN2014-53772 and TIN2017-85572-P. The second author was also supported by grants TIN2014-58662-R and DPI2017-86372-C3-3-R (MINECO/AEI/FEDER, UE).

7 References

[1] Wang, Q., Fu, X., Zhang, X.P., *et al.*: 'A fusion-based method for single backlit image enhancement'. 2016 IEEE Int. Conf. on Image Processing (ICIP), Arizona, USA, 2016, pp. 4077–4081
[2] Fu, X., Zeng, D., Huang, Y., *et al.*: 'A fusion-based enhancing method for weakly illuminated images', *Signal Process.*, 2016, **129**, pp. 82–96
[3] Li, Z., Wu, X.: 'Learning-based restoration of backlit images', *IEEE Trans. Image Process.*, 2018, **27**, (2), pp. 976–986
[4] Land, E.H.: 'The retinex', *Am. Sci.*, 1964, **52**, (2), pp. 247–264
[5] Land, E.H.: 'The retinex theory of color vision', *Sci. Am.*, 1977, **237**, pp. 108–128
[6] Jobson, D.J., Rahman, Z., Woodell, G.A.: 'A multiscale retinex for bridging the gap between color images and the human observation of scenes', *IEEE Trans. Image Process.*, 1997, **6**, (7), pp. 965–976
[7] Petro, A.B., Sbert, C., Morel, J.M.: 'Multiscale retinex', *Image Process. On Line*, 2014, **4**, pp. 71–88
[8] Rizzi, A., Gatta, C., Marini, D.: 'A new algorithm for unsupervised global and local color correction', *Pattern Recognit. Lett.*, 2003, **24**, (11), pp. 1663–1677
[9] Getreuer, P.: 'Automatic color enhancement (ACE) and its fast implementation', *Image Process. On Line*, 2012, **2**, pp. 266–277
[10] Lisani, J.L., Petro, A.B., Sbert, C.: 'Color and contrast enhancement by controlled piecewise Affine histogram equalization', *Image Process. On Line*, 2012, **2**, pp. 243–265
[11] Limare, N., Lisani, J.L., Morel, J.M., *et al.*: 'Simplest color balance', *Image Process. On Line*, 2011, **1**, pp. 297–315. https://doi.org/10.5201/ipol.2011.llmps-scb
[12] Drago, F., Myszkowski, K., Annen, T., *et al.*: 'Adaptive logarithmic mapping for displaying high contrast scenes'. Proc. of EUROGRAPHICS, Granada, Spain, 2003, vol. 22,
[13] Reinhard, E., Devlin, K.: 'Dynamic range reduction inspired by photoreceptor physiology', *IEEE Trans. Vis. Comput. Graphics*, 2005, **11**, (1), pp. 13–24
[14] Mai, Z., Mansour, H., Mantiuk, R., *et al.*: 'Optimizing a tone curve for backward-compatible high dynamic range image and video compression', *IEEE Trans. Image Process.*, 2011, **20**, (6), pp. 1558–1571
[15] Zuiderveld, K.: 'Contrast limited adaptive histogram equalization', In: Heckbert, P.S. (Ed.): '*Graphic gems IV*' (Academic Press Professional, USA, 1994), pp. 474–485, ISBN: 0–12-336155-9
[16] Caselles, V., Lisani, J.L., Morel, J.M., *et al.*: 'Shape preserving local histogram modification', *IEEE Trans. Image Process.*, 1999, **8**, (2), pp. 220–230
[17] Lisani, J.L.: 'An analysis and implementation of the shape preserving local histogram modification algorithm', *Image Process. On Line*, 2018, **8**, pp. 408–434
[18] Moroney, N.: 'Local color correction using non-linear masking'. IS&T/SID Eight Color Imaging Conf., Arizona, USA, 2000, pp. 108–111
[19] Salas, J.G.G., Lisani, J.L.: 'Local color correction', *Image Process. On Line*, 2011, **1**, pp. 260–280
[20] Lisani, J.L.: 'Adaptive local image enhancement based on logarithmic mappings'. IEEE Int. Conf. on Image Processing (ICIP), Athens, Greece, 2018, pp. 1747–1751
[21] Durand, F., Dorsey, J.: 'Fast bilateral filtering for the display of high-dynamic-range images', *ACM Trans. Graph.*, 2002, **21**, (3), pp. 257–266
[22] Fattal, R., Lischinski, D., Werman, M.: 'Gradient domain high dynamic range compression', *ACM Trans. Graph.*, 2002, **21**, (3), pp. 249–256
[23] Mertens, T., Kautz, F.V.R. J.: 'Exposure fusion'. Proc. of 15th Pacific Conf. on Computer Graphics and Applications, Hawaii, USA, 2007, pp. 382–390
[24] Deng, G.: 'A generalized unsharp masking algorithm', *IEEE Trans. Image Process.*, 2011, **20**, (5), pp. 1249–1261
[25] Ancuti, C.O., Ancuti, C., Bekaert, P.: 'Enhancing by saliency-guided decolorization'. 2011 IEEE Conf. on Computer Vision and Pattern Recognition, 2011, pp. 257–264
[26] Morel, J.M., Petro, A.B., Sbert, C.: 'Automatic correction of image intensity nonuniformity by the simplest total variation model', *Methods Appl. Anal.*, 2014, **21**, (1), pp. 107–120
[27] Morel, J.M., Petro, A.B., Sbert, C.: 'Screened Poisson equation for image contrast enhancement', *Image Process. On Line*, 2014, **4**, pp. 16–29
[28] Hessel, C.: 'An implementation of the exposure fusion algorithm', *Image Process. On Line*, 2018, **8**, pp. 369–387
[29] Ma, K., Li, H., Yong, H., *et al.*: 'Robust multi-exposure image fusion: A structural patch decomposition approach', *IEEE Trans. Image Process.*, 2017, **26**, (5), pp. 2519–2532
[30] Kou, F., Li, Z., Wen, C., *et al.*: 'Multi-scale exposure fusion via gradient domain guided image filtering'. 2017 IEEE Int. Conf. on Multimedia and Expo (ICME), Hong Kong, 2017, pp. 1105–1110
[31] Mittal, A., Soundararajan, R., Bovik, A.C.: 'Making a completely blind image quality analyzer', *IEEE Signal Process. Lett.*, 2013, **20**, (3), pp. 209–212
[32] Martorell, O., Sbert, C., Buades, A.: 'Ghosting-free dct based multi-exposure image fusion', *Signal Process., Image Commun.*, 2019, **78**, pp. 409–425